The effect of linker histones on force-induced nucleosome unstacking

THESIS

submitted in partial fulfillment of the
requirements for the degree of

BACHELOR OF SCIENCE
in
PHYSICS

Author :	Sven Schoonebeek
Student ID :	1692070
Supervisor :	John van Noort
2^{nd} corrector :	Thomas Schmidt

Leiden, The Netherlands, September 2, 2019

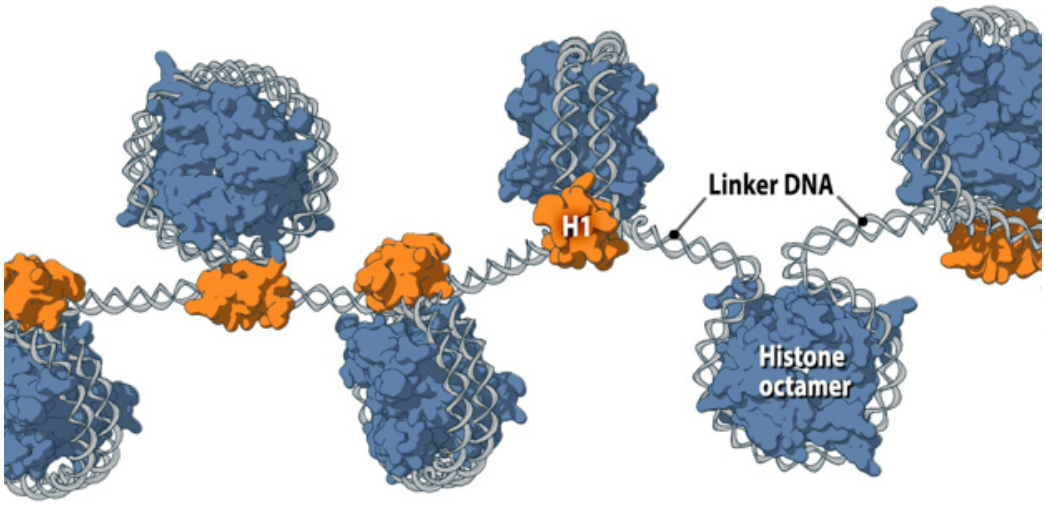

[1]

The effect of linker histones on force-induced nucleosome unstacking

Sven Schoonebeek

Gorlaeus Faculty Office
Einsteinweg 55, 2333 CC Leiden, The Netherlands

September 2, 2019

Abstract

The structure of chromatin plays a vital role in the regulation of gene expression. In this thesis, the mechanical properties of chromatin are investigated by measuring force-extension curves with Magnetic Tweezers. Two models are re-introduced that accurately describe these curves. Upon adding linker histone H1, a protein that can bind to individual nucleosomes, stabilization of nucleosome unstacking up to 10 pN was observed. Varying the Nucleosome Repeat Length (NRL) of the chromatin fibers with linker histones resulted in different degrees of stabilization: 168NRL fibers have a higher energy barrier for unstacking than 197NRL fibers. This could be caused by increased nucleosome stiffness at lower NRLs. This difference could have an important effect on transcription regulation in vivo.

Contents

Chapter 1

Introduction

1.1 Genomic architecture

In eukaryotes, genetic information is stored in the cell nucleus as DNA. The complete human genome contains approximately 3 *Gbp* of DNA [8], which equals a stretched length of over 1 meter. Storing genetic information in an unfolded manner would impart efficient gene localization and transcription regulation. Moreover, DNA would be more vulnerable for damage. In order to store genetic information in an efficient and organized way, DNA is subjected to several folding mechanisms [9]. At the primary level, 146 basepairs (bp) of DNA are wound left-handed 1.65 times around a histone octamer core. The histones are a family of highly alkaline proteins, which enables them to buffer changes in environmental acidity [10]. The histone octamer (HO) consists of a H3-H4 tetramer and two H2A-H2B dimers, where H3, H4, H2A and H2B are the canonical core histones. The DNA-HO complex is called a nucleosome [11]. Approximately 50 *bp* of DNA seperates the individual nucleosomes, the linker DNA. The structure of chromatin has been researched by electron microscopy (EM). However, the structure is highly dynamic and is mainly influenced by interactions between nucleosomes [16]. This makes a structural analysis with EM difficult.
A mechanical approach using Magnetic Tweezers proves to be more fruitful. Nucleosomes can stack into a higher order configuration called a 30 *nm* chromatin fiber. Torsional and translational stress acting on chromatin fibers alters their configuration, revealing an equilibrium situation at low forces and an irreversible, stepwise unwrapping of nucleosomes at higher forces [3]. In this thesis, two models will be re-introduced to ana-

lyze the low force equilbrium regime and the high force non-equilibrium regime.

1.2 The nucleosome: a dynamic structure

The structure of the nucleosome has already been investigated extensively, and has been shown to be highly dynamic just like chromatin. For example, nucleosomes can spontaneously unwrap part of their DNA from the HO [12]. These nucleosome dynamics are closely related to transcription modulation, and alterations to nucleosome structure can therefore affect DNA accessibility. There are three known ways in which the nucleosome structure can be altered. First, histones can be chemically altered by histone modification enzymes which will change the free energy landscape of HO-DNA interactions [13][15]. A few well-known enzymatic alterations include methylation, acetylation, ubiquitylation and phosphorylation of histones. Second, the spontaneous wrapping and unwrapping behavior enables nucleosomes to regulate occupancy of DNA-binding proteins. When the nucleosome unwraps, there will be more binding sites for the protein to bind to, increasing DNA accessibility [12]. Finally, the nucleosome can be altered by substitution of canonical core histones by histone variants. Histone variants that lack an acidic patch impede nucleosome stacking, which improves accessibility but also leaves the unwrapped DNA unprotected [14].

1.3 Linker histones

A fifth type of histone protein variants that can interact with the HO are the linker histones (LH). Unlike canonical histones, the linker histones do not wrap DNA but instead bind to the core and the linker DNA. The LH-HO structure is called a chromatosome, and the abundance of chromatosomes is approximately equal to that of nucleosomes in eukaryotic cells [18]. Two known linker histones are H1 and H5, where the major difference between these two histones lies in the binding site at the core octamer. The on-dyad binding of H5 allows the fiber to fold more densely, while the off-dyad binding of H1 leaves the fiber in a less dense configuration [17].

Because the linker histones bind to the linker DNA they have a major influence in higher order fiber structure. Specifically, the linker histones can facilitate binding of the linker DNA, which further condenses the fiber into a zig-zag structure [19]. Magnetic Tweezers have been sparingly used to study the mechanical properties of chromatin consisting of stacked chromatosomes. Further work is needed on how LH affects the stability of chromatin fibers. Therefore, the goal of this thesis will be to identify the role of linker histones in nucleosome stacking.

Chapter 2

Theory

2.1 Statistical mechanics

To study the mechanical properties of chromatin fibers, models will be introduced to analyze chromatin fibers with and without linker histone H1. To analyze the force-extension curves of chromatin without H1, a model based on statistical mechanics is used. Statistical mechanics is a powerful tool that allows for description of systems in thermodynamic equilibrium consisting of a large number of components.

Because the chromatin fiber can be in a large number of states during the experiments, but will remain in thermodynamic equilibrium when low forces are applied and transitions are reversible, use of statistical mechanics is justified. The equation that will be used is the Maxwell-Boltzmann equation, which describes the average distribution of non-interacting particles in different states, in a system which is in thermal equilibrium:

$$P_{state} = \frac{D_{state} \cdot \exp\left(\frac{-G_{state}}{k_B T}\right)}{\sum\limits_{states} D_{state} \cdot \exp\left(\frac{-G_{state}}{k_B T}\right)} \tag{2.1}$$

In this equation, P_{state} is the probability that a component will be in a certain state, G_{state} is the free energy of that state ($k_B T$), D_{state} is a factor that accounts for the degeneracy of that state and k_B is the Boltzmann factor.

When probing the force-extension relation for chromatin fibers, the Maxwell-Boltzmann equation will be used to calculate the average extension of the fiber. This can only be done when the extension of a single nucleosome in all states is known. Since the nucleosome consists of wrapped DNA around the histone octamer, the force-extension behavior of DNA is

Conformation	$L_{wrap}(bp)$	$L_i(bp)$	$\Delta G_{conformation}(k_BT)$
Fully wrapped	147	$NRL - L_{wrap}$	0
Partially unwrapped	107	$NRL - L_{wrap}$	g_1
Singly unwrapped	80	$NRL - L_{wrap}$	$g_1 + g_2$
Fully unwrapped	-	NRL	$g_1 + g_2 + g_3$

Table 2.1: *Used constants of the four different nucleosome conformations. The free energies of the transitions are roughly $g_1 = 19 \pm 2k_BT$, $g_2 = 4.4 \pm 0.7k_BT$ [3]. g_3 does not belong to an equilibrium transition and is manually derived.*

important. It is already known that DNA extends under force according to a worm-like chain [2]:

$$z_{WLC}(f, L) = L\left(1 - \frac{1}{2}\sqrt{\frac{k_BT}{fA}} + \frac{f}{S}\right) \tag{2.2}$$

In this equation, the contour length L is the total length of the DNA strand in basepairs (bp), f is the applied force (pN), A is the persistence length of the strand (nm), and S is the stretch modulus (pN). The corresponding free energy (k_BT) can now be calculated by integrating the extension over the force:

$$G_{WLC}(f, L) = -\int_0^f z_{WLC}(\tilde{f}, L)\, d\tilde{f} = -L\left(f - \sqrt{\frac{fk_BT}{A}} + \frac{f^2}{2S}\right) \tag{2.3}$$

Chromatin fibers consist of single nucleosomes that can be in four different conformations when they are subject to external force, as found by Meng et al [3]: a fully wrapped conformation, a partially unwrapped conformation, a singly unwrapped conformation, and a fully unwrapped conformation. Every conformation unwraps some DNA from the histone octamer, which allows defining the contour length of this released free DNA. The contour lengths for the different conformations can be found in table 2.1, and a schematic overview of the different conformations is visualized in figure 2.1.

The different conformations of each nucleosome will extend under force according to 2.2. This allows for calculation of the extension for each conformation:

$$z_{conformation}(f) = z_{WLC}(f, L_i) \tag{2.4}$$

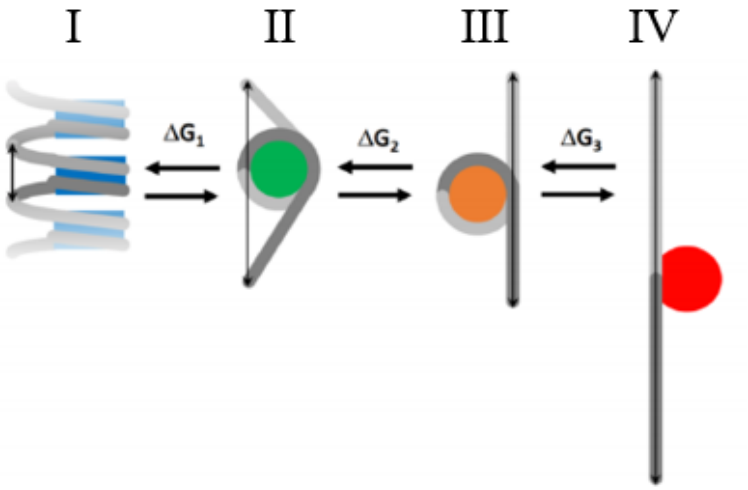

Figure 2.1: *The four different nucleosome conformations as proposed by Meng et al [3]: fully wrapped (I), partially unwrapped (II), singly unwrapped (III) and fully unwrapped (IV). The free energies of the transitions can be found in table 2.1. This figure was obtained from Kaczmarczyk [7].*

Each unwrapping event is also accompanied by a change in free energy ΔG, which is added to the free energy of the conformation:

$$G_{conformation}(f) = G_{WLC}(f, L_i) + \Delta G_{conformation} \tag{2.5}$$

The different free energies corresponding to the transitions between conformations can be found in table 2.1.

Under lowest force, when nucleosomes are still arranged in a fiber, the linker DNA is constrained. This reduces the extension for each nucleosome, which makes equation 2.4 non-applicable. It was found empirically that when all nucleosomes are stacked, the fiber behaves like a Hookean spring with fiber stiffness k (pN/nm) [22]. Thus, the first conformation is best descibed by Hooke's Law:

$$z_{fiber}(f) = \frac{f}{k} + z_0 \tag{2.6}$$

$$G_{fiber}(f) = \frac{f^2}{2k} \tag{2.7}$$

In Magnetic Tweezers, the extension of a fiber is obtained from measuring the height of a bead that is bound to the chromatin fiber. Since the chromatin fiber is usually not exactly bound to the bottom of a bead an offset z_0 is added to the fiber extension.

The fiber can now be in a $state = n_1, n_2, n_3, n_4$, where there are n nucleosomes in conformation i. Consequently, each state has a corresponding state extension which can be calculated by summing over the contributions of all nucleosomes in each conformation, and adding the extension of the DNA handles at the flanks of the fiber:

$$z_{state}(f) = \sum_i n_i z_i + z_{WLC}(f, L_{handles}) \tag{2.8}$$

$$G_{state}(f) = \sum_i n_i G_i + G_{WLC}(f, L_{handles}) \tag{2.9}$$

The probability that a nucleosome will be in conformation i at a certain force f follows the Maxwell-Boltzmann distribution 2.1. Because some states can have the same free energy, a degeneracy factor calculated from a binomial distribution is needed to correct for this:

$$D_{state} = \prod_{i<j} \binom{n_i + n_j}{n_i} \tag{2.10}$$

Now the average extension of the whole fiber can be calculated by combining equations 2.8, 2.10 and 2.1, including the extension, degeneracy and probability of each state:

$$\langle z_{tether}(f) \rangle = \sum_{states} z_{state}(f) \cdot D_{state} \cdot P_{state} \tag{2.11}$$

This allows for the complete modelling of the chromatin fiber at all forces when the tether is in thermal equilibrium and transitions are all reversible.

2.2 Nucleosome dynamics

2.2.1 High-force nucleosome unwrapping

At forces above 10pN, the fiber enters a non-equilibrium regime characterized by the stepwise unwrapping of nucleosomes. The unwrapping is irreversible and can therefore not be described by the statistical mechanics model discussed in previous section. Still, the fiber can be in discrete states, whose extension can be calculated by equation 2.8. The stepwise unwrapping observed at high forces can therefore be described by calculating the probability that a data point i belongs to a certain state. By

using a Z-score to quantify the deviation of the state extension z_{state} from the measured value $z(f)$ [3] [7]:

$$Z_i(f) = \frac{|z_i(f) - z_{state}(f)|}{\sigma(f)} \tag{2.12}$$

Where σ is the expected standard deviation (nm), which is the quadratic sum of the measurement error and the thermal fluctuations:

$$\sigma^2 = \sigma^2_{measurement} + \sigma^2_{thermal} \tag{2.13}$$

The measurement error depends on the mechanical background vibarations and accuracy of the bead tracking software, and the standard deviation in thermal fluctuations can simply be calculated from the equipartition theorem $\frac{1}{2}k_BT = \frac{1}{2}k\sigma^2_{thermal}$. The local stiffness k (pN/nm) is the stiffness of the tether evaluated for a single state, and depends on the force:

$$k = \frac{z_{state}\,(f + df) - z_{state}\,(f)}{df} \tag{2.14}$$

Where $z_{state}\,(f)$ is the extension of a state at force f calculated by equation 2.8. The probability P_i that data point j belongs to a state i is then calculated from the normal distribution by using the error function:

$$P_i(f) = 1 - \mathrm{erf}\,(Z_i(f)) \tag{2.15}$$

To obtain the probability landscape, equation 2.15 is summed over all data points $P_i(f)$ for all possible states in the entire measured force-extension curve. The peaks in the probability landscape correspond to the states that most likely belong to stable unwrapping intermediates. Only states with a minimum of two datapoints were further processed.

Merging states

Implementing the Z-score analysis mentioned above often resulted into groups of datapoints which appeared wrongly divided into multiple nearby states. To correct for this, multiple states were merged, using the weighted average of neighboring states when the following criteria were met [20]:

1. Each of two original states must have at least 50% of the datapoints within 2σ of the probability distribution of the merged state.
2. At least 80% of the datapoints must lie within 2σ of the merged probability distribution.

Version of September 2, 2019– Created September 2, 2019 - 12:50

When these conditions were met, the datapoints are attributed to the merged state.

2.2.2 Non-equilibirium nucleosome unstacking

When linker histones are added to the chromatin fibers, force-extension curves show discrete unstacking steps below $10pN$. This indicates that the unfolding of the chromatin fiber is no longer in thermodynamic equilibrium. The probability landscape obtained from equation 2.15 can also be used to identify these discrete states. However, important parameters of interest, such as the free energy change of the transition, cannot be calculated with equation 2.15. Instead, the transition rates between different conformations need to be taken into account explicitly.

Nucleosomes can spontaneously wrap (closed state) or unwrap their outer turn of DNA (open state), changing their conformation. The forward and backward rates at which this happens depends on the free energy difference between two conformations i, j and is described by the Arrhenius equation:

$$k_{ij} = k_0 \exp\left(-\left(\frac{\Delta G_{ij} - fz}{k_B T}\right)\right) \tag{2.16}$$

Where k_0 is the initial rate of passing the energy barrier (s^{-1}) and ΔG_{ij} is the free energy difference between the conformations in the direction ij. k_0 is related to the rupture force of a nucleosome F^* and the extension at the highest energy barrier of the transition Δz by [4][20]:

$$F^* = \frac{k_B T}{\Delta z}\left(\ln\left(\frac{1}{N}\frac{dF}{dt}\right) - \ln\left(k_0 \frac{k_B T}{\Delta z}\right)\right) \tag{2.17}$$

Where additional parameters are the number of nucleosomes left that are still in the closed state N, and the pulling rate $\frac{dF}{dt}$. By plotting rupture-forces as a function of the logarithm of the pulling rate in a similar fashion to Brower-Toland et al [4], insightful parameters such as k_0, ΔG_{ij} and Δz are recovered. Because the probability of a rupture will increase with decreasing N, the logarithm in these plots is corrected by the nucleosome ratio factor:

$$\frac{N_o - N}{N} \tag{2.18}$$

Where N_o is the number of nucleosomes in the open state.

Version of September 2, 2019– Created September 2, 2019 - 12:50

2.2.3 Single molecule force spectroscopy

Magnetic Tweezers is a technique to manipulate single molecules by using single molecule force spectroscopy. The paramagnetic beads are subjected to an external magnetic force which will pull on the attached chromatin molecule. The biggest advantage of using magnetic tweezers over other force spectroscopy techniques, such as optical tweezers or atomic force microscopy, is the possibility to acquire data from multiple molecules at once [6]. A custom built setup was used to utilize the Magnetic Tweezer technique to generate force-extension curves of chromatin. The setup uses LED light (Lumitronix) to illuminate a sample of tethered beads. Diffracted light was collected by an oil-immersion objective (Olympus) and collected with a CMOS camera at 30 Hz. A more detailed description of the setup is provided by Kruithof et al [21], and a schematic overview of the setup is shown in figure 2.2. A LED is used to illuminate the beads imaged by a microscope, which will produce a diffraction pattern when the light of the LED falls through the objective. When a bead moves out of focus, the diffraction pattern will shift. This shift with respect to the focus is correlated to a reference image to obtain the change in position of the bead. This allows for nanometer-accurate position measurements in 3D. By lowering the magnet to the sample, it will increase the magnetic force on the bead. The magnetic force on the M270 2.8 μm beads was related to the vertical position of the magnet by fitting a double exponential function to it *:

$$F(z) = 85 \cdot \left(0.7 \cdot \exp\left(\frac{-z}{1.4}\right) + 0.3 \cdot \exp\left(\frac{-z}{0.8}\right)\right) + 0.01 \tag{2.19}$$

*This was done by Nicolaas Hermans from Leiden University

Version of September 2, 2019– Created September 2, 2019 - 12:50

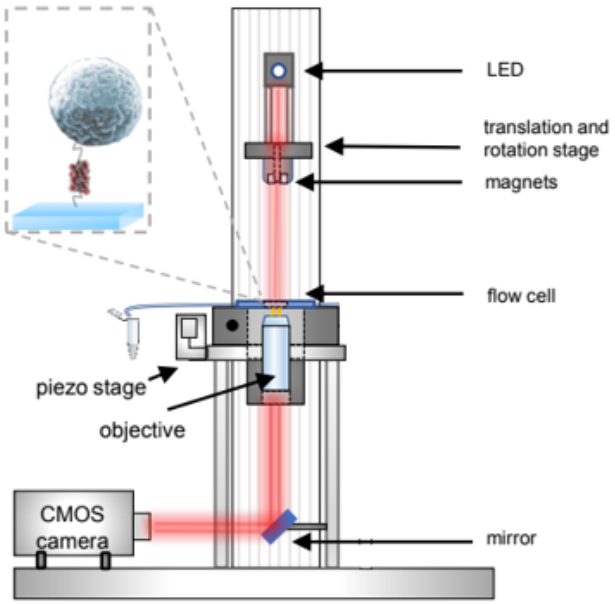

Figure 2.2: *Setup of the custom built Magnetic Tweezers. A LED illuminates the sample and diffracted light is collected by the objective. The focused beam is projected onto the CMOS camera. The setup also contains a piezo stage for phase calibration, and a rotational motor which was not used in this thesis. This figure was obtained from Kaczmarczyk [7] and altered.*

Chapter 3

Methods

3.1 Methods

3.1.1 Flowcell preparation

A flowcell consists of small channels running between two slides of glass mounted on a frame. By flushing the sample into one of the channels individual chromatin fibers can be tethered between on of the slides and a paramagnetic bead. spectroscopy can be performed on the sample. The following protocol was used to prepare flowcells for measuring in the Magnetic Tweezers [7].

1. Preparing the frame.

   For new flowcell frames: put a 3 *mm* silicone tubing through the big holes in the flowcell. Use a scalpel to cut off the silicone tubing at the surface of the frame.

   For used flowcell frames: remove the sticker and glass by rinsing the frame with acetone.

   Clean the frame and flush all holes with acetone. Dry the frame and channels thoroughly with nitrogen gas.

2. Cleaning the coverslips.

   Immerse 24 x 60 mm coverslips in isopropanol and sonicate for a minimum of 10 minutes in the ultrasonic cleaner. Immerse the 24 x 40 mm coverslips in isopropanol for 10 minutes. Afterwards dry the coverslips with a stream of N2 gas.

3. Printing the flowcell channels.

Put a single-sided sticker strip on the Cameo Silhouette sheet. Select the custom template containing (multiple) holes on both sides connected by (multiple) channels. After the cutting is done, put a double-sided sticker strip on the sheet and select the custom template containing only the channel(s).

4. Assembling the flowcell.

   Put the single-sided sticker with the holes on the frame, on the side with the big holes. The holes on the frame should overlap with the holes on the sticker. Turn the frame around and put the 24x40 mm coverslip on the sticker. Again, turn around and put the double-sided sticker on the single-sided sticker. The channels on both stickers should overlap. Finally, put the 24x60 mm coverslip on the double-sided sticker. Use a pipettetip to gently push both coverslips against the stickers.

5. Incubation with anti-digoxigenin.

   Prepare 150 of 10 $ng/$ anti-digoxigenin dissolved in filtered phosphate-buffered saline (PBS) solution. Flush 150 into the flowcell, seal the channels with tape, and incubate for 2 hours at 4°C. When there are multiple channels, divide 150 anti-digoxigenin solution equally over the channels. Prepare new 10 $ng/$ anti-digoxigenin solution for every flowcell assembly. Do not put the anti-digoxigenin solution on the vortex. Mix slowly with a pipette, such that no bubbles arise.

6. Flowcell passivation.

   Prepare 150 of 4% BSA (bovine serum albumin), 0.1% Tween-20 solution dissolved in HPLC water. Flush 150 of the 4% BSA solution into the flowcell, seal the channels with tape and incubate for 2 hours at 4°C. When there are multiple channels, divide 150 4% BSA solution equally over the channels. Prepare new 4% BSA solution for every flowcell assembly. Do not put the BSA solution on the vortex. Mix slowly with a pipette, such that no bubbles arise. The flowcell can be stored for up to one week at this point.

7. Washing the flowcell.

   Prepare the 10x pre-ESB buffer (compounds can be found in table 3.1). Dilute to 1x ESB(+) buffer for chromatin (according to table 3.2). Flush 500μL of ESB(+) buffer into the flowcell. When there are multiple channels, divide 500μL ESB(+) buffer equally over the channels. Prepare new ESB(+) buffer for every flowcell assembly.

Component	Amount	Final concentration
KCl	37.28 g	1 M
NaN_3	3.25 g	100 mM
Tween-20	5 mL	1%
1M HEPES pH 7.5	50 mL	100 mM
HPLC water	445 mL	

Table 3.1: *The components for preparation of 1 L of 10x pre-ESB buffer.*

Component	Amount	Final concentration
10x pre-ESB buffer	1 mL	10%
20 mM $MgCl_2$	1 mL	2 mM
4% BSA in HPLC water	0.5 mL	0.2%
HPLC water	7.5 mL	

Table 3.2: *The components for preparation of 10 mL of ESB(+) buffer.*

The 10x pre-ESB buffer can be stored for maximally 1 month at 4°C.

8. Preparing the sample.

   Add approximately 20 ng of reconstituted chromatin fibers to 500 μL of ESB(+) buffer. Mix very gently with a pipette. Flush all 500 μL gently into the flowcell. When there are multiple channels, divide the 500 μL equally over the channels. One should consider flushing the chromatin into the channels in seperated measurement rounds, as this allows for more measurements per flowcell. Incubate for 10 minutes at room temperature.

9. Adding magnetic beads

   Vortex Thermo Fischer Invitrogen Dynabeads M-270 Streptavidin (10 mg/mL) for 1 minute. Add 1 μL of beads to 500 μL of ESB(+) buffer for chromatin. When doing measurements with the linker histone, add 50 ng human H1 to the bead-buffer mixture and mix gently with a pipette. Flush in 500 μL or equally divided parts into the channel(s), with a flowrate not exceeding 100μL/min to prevent sample degradation. Incubate for another 10 minutes a room temperature.

3.1.2 Magnetic Tweezers

By relating the bead heigth to the force, a force-extension curve can be obtained for single chromatin tethers. The bead diffraction pattern was analyzed by using a 3D FFT tracking algorithm developed by Brouwer et al (Leiden University, in preparation). The following protocol describes how measurements were done using the setup [7]. The protocol is visualized in figure 3.1.

1. Cleaning and immersing the objective.
   Clean the objective by using lens paper. Immerse the objective in a drop of oil.

2. Calibration of the magnet position.
   Align the position of the magnet such that the longitudinal axis of the magnet is perpendicular to the longest side of the flowcell. Place a flowcell that has already been measured in the setup. Alternatively, it is possible to use the measurement flowcell for calibration, which will make the area near the magnet (along the longitudinal axis) unusable for measurements, because it exposes tethers to high force. Start the setup: motors, LED and camera. Bring a single bead into focus using PageUp/PageDown (+ Shift) keys. Lower the magnet towards the top coverslip, until it just touches the glass. The bead diffraction pattern will change as a response to the slight bending of the glass. Move the magnet upwards in small (0.01 mm) steps, until the diffraction pattern returns to the initial state. The position of the magnet is calibrated as 0 mm by clicking the 'reset' button in the LabVIEW interface. Move the magnet 15mm up. Remove the old flowcell and mount the measurement flowcell on the setup (when the measurement flowcell was used for calibration, move the magnet one width along its transversal axis).

3. Calibration of the camera focus.
   Find beads in the field of view (FOV) by clicking the 'find' button in the LabVIEW interface. Zoom in on a bead that is stuck at the surface of the flowcell. There should not be any visible movement of the bead. Bring the bead into focus by using PageUp/PageDown (+ Shift) keys. The bead is in focus when the diffraction rings disappear. Click the 'calibrate' button in the LabVIEW interface to calibrate camera focus. The phase diagram should display two straight crossing lines. When this is not observed, recalibrate with a different stuck bead.

Version of September 2, 2019– Created September 2, 2019 - 12:50

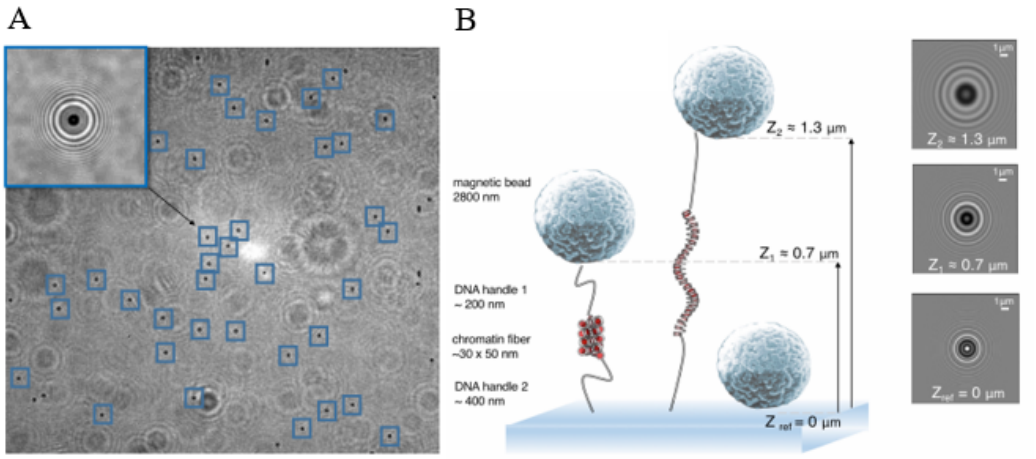

Figure 3.1: *Finding and selecting beads with the LABVIEW software.* ***A****: a 3D FFT LABVIEW bead tracking algorithm developed by Brouwer et al (Leiden University, in preparation) is used to detect bead diffraction patterns.* ***B****: the diffraction pattern depends on the vertical position of the bead. The diffraction pattern shift can therefore be related to the change in vertical position of the bead, which is the core of single molecule force spectroscopy. This figure was obtained from Kaczmarczyk [7] and altered.*

4. Selecting beads.

   Select or unselect beads by using Alt + Click. Unselect all beads at the corners of the FOV, clustered beads and beads that are moving out of their region of interest (ROI). If necessary, the ROI can be expanded a bit.

5. Executing the measurement.

   Select or create a magnet trajectory. When selected, click 'run'. The trace will be executed by the LabVIEW program. When done, the position data will be automatically saved by the LabVIEW program. To do another measurement, move the magnet ¿5 mm along its transversal axis.

3.1.3 Sample preparation

The chromatin was reconstituted on DNA containing an array of 601 Widom nucleosome positioning sequences. This sequence defines the Nucleosome Repeat Length of the resulting chromatin. Here, arrays with 16 times 168NRL and 197NRL were used. The DNA was labelled with biotin and

Figure 3.2: *Bare DNA or chromatin fibers labelled with biotin and digoxigenin can bind to steptavidin and anti-digoxigenin groups. This figure was obtained from Janissen et al [23] and altered.*

digoxigenin because it needs to have two distinct binding sites: one for the streptavidin group on the bead and one for the anti-digoxigenin antibody on the surface of the flowcell. Steptavidin has a very high affinity for biotin [23]. Figure 3.2 shows a schematic overview of the biotin-digoxigenin binding. DNA strands were digested using BsaI and BseYI enzymes (NE BioLabs). The digested DNA was labelled on the BsaI site with digoxigenin-11-ddUTP in presence of dCTP (Roche Diagnostics), and the BseYI site was labelled with biotin-16-ddUTP in presence of dGTP (Roche Diagnostics). Both labels were incorporated using Klenow fragments and Klenow reaction buffer.

The digested and labelled DNA was dissolved in a high salt buffer (2.5M NaCl, 1xTE) along with human recombinant histone octamer (EpiCypher) and pipetted into tubes with a membrane bottom. The DNA:HO ratio was varied from 1 to 2 over five different tubes to make sure the right amount of nucleosomes were formed in at least one tube. DNA-HO was the incubated overnight at 4°C while a low salt buffer (1xTE) was pumped into the beaker at a rate of 0.9 ml/min. Mixed buffer was drained from the beaker at the same rate. The five different tubes were the stored at 4°C for a maximum of five weeks [20] [7] *.

*These reconstitutions were done by Chi Pham of Leiden University

Chapter 4

Results

4.1 Flowcell protocol optimalization

Before doing measurements on chromatin, the flowcell preparation protocol stated in the previous section was optimized for force-extension measurements on DNA. Four different protocols were compared. The beads were first classified as either stuck or tethered (figure 4.1A). The tethered beads were divided into traces that rupture, traces that could be fitted with a WLC (equation 2.2), and beads showing behaviour that could not be identified (other). This is shown in figure 4.1B. The best protocol is the protocol yielding the most beads that could be fitted to a WLC.

Figure 4.1B shows that the differences in quality curves between the protocols are very small. Therefore, the fastest (4 hours of total incubation time) and most cost-effective (10ng/μL anti-digoxigenin) protocol was used for doing measurements on chromatin.

4.2 Chromatin

Reconstituted chromatin fibers were measured in the Magnetic Tweezers with and without adding H1. Data analysis was done with custom written Python software in 5 steps:

1. The offset of the bead was determined by fitting a worm-like chain (equation 2.2) to the datapoints above 20pN of the release curve.

2. For chromatin without H1, the statistical mechanics model (equation 2.11) was fitted to the datapoints below 7pN of the pulling curve.

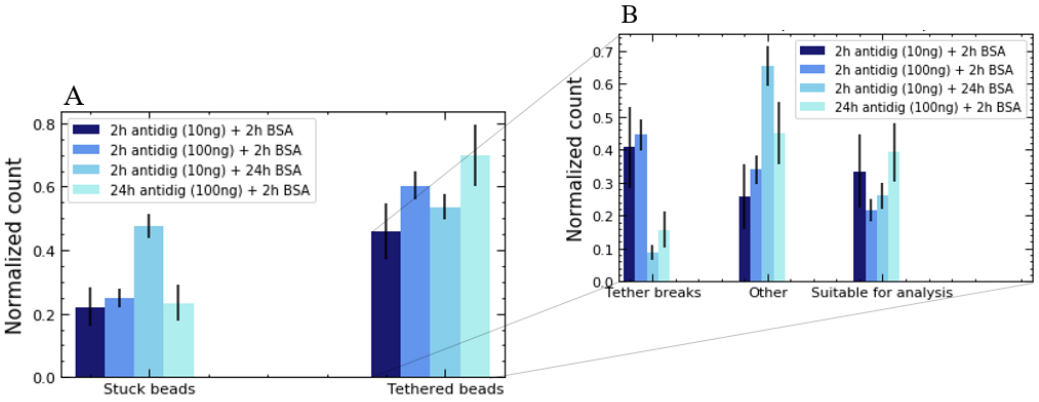

Figure 4.1: *2 hour incubation with antidig (10ng/μL) followed by 2 hour incubation with 4% BSA solution is the best flowcell protocol for DNA force-extension measurements.* ***A****: number of stuck beads and tethered beads (figure 7.2) as a fraction of the total beads.* ***B****: Number of tether ruptures, beads suitable for analysis and other as a fraction of the total number of tethered beads. The suitable for analysis criterium was used to determine the best protocol by fitting extendable WLC's (figure 7.1) to the data. Since the difference in quality curves between the different protocols is very small, the fastest and most cost-effective protocol was deemed best.*

The fitting parameters are the total number of nucleosomes N_{tot}, the total number of tetrasomes N_{tet}, the free energy difference of the first transition g_1 and the stiffness of the fiber k. The free energy of the second transition $g2$, was fixed at $5.5k_BT$. The bead offset value z_0 from previous step was used as a fixed parameter.

3. For chromatin with H1, the statistical mechanics model cannot be used, because the observed transitions at forces below $10pN$ for chromatin with H1 are not in thermal equilibrium. A low force comparison between chromatin with H1 and chromatin without H1 is shown in figure 4.2.

   Instead, the probability landscape (equation 2.15) was used to identify discrete states. Figure 4.3 shows identification of unstacking steps with the t-test model in chromatin with H1. The low force boundary was set at a higher value (10-12pN) than the 7pN used for chromatin in equilibrium.

4. The last step was to fit the high force regime of the pulling curve (every data point above the low force boundary set in the previous

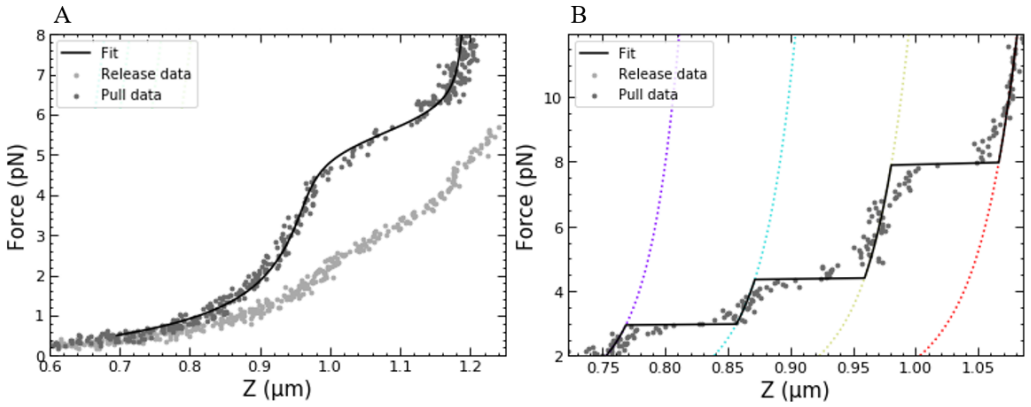

Figure 4.2: *At forces below 7pN, chromatin fibers without H1 unfold in thermal equilibrium, whereas chromatin fibers with H1 show non-equilibrium, discrete unstacking steps.* ***A****: the equilibrium model describes chromatin fibers without H1 at forces below 7pN. The fitting parameters used for this fiber are:* $N_{tot} = 14.0 \pm 0.1$, $N_{tet} = 0.9 \pm 0.4$, $g_1 = 8.3 \pm 0.3 k_B T$, $k = 0.1 \pm 0.1 pN/nm$. g_2 *was fixed at* $5.5 K_B T$. ***B****: Unstacking behaviour in fibers with H1 at forces below 10pN. Datapoints are clustered and can be described by identifying discrete states using the t-test model.*

step). Equation 2.15) was also used to identify the unwrapping steps. Criteria mentioned in section 2.2.1 were used to merge the states. The identification of states before and after merging states is shown in figure 4.4.

5. The different regimes were concatenated to get the complete force-extension curve. Completely fitted force-extension curves of chromatin with H1 and without H1 are shown in figure 4.5. Typically, the yield of such curves was only about 5 % of the total number of beads, the biggest problem being the rupturing of tethers at forces above 20pN.

6. Unstacking and unwrapping behaviour was further analyzed using the method described in section 2.2.2. A plot of the rupture forces as a function of the logarithm of the pulling rate, corrected with the ruptured nucleosome ratio given by equation 2.18, is shown in figure 4.6D for unwrapping events, and in figure 4.7 for unstacking events.

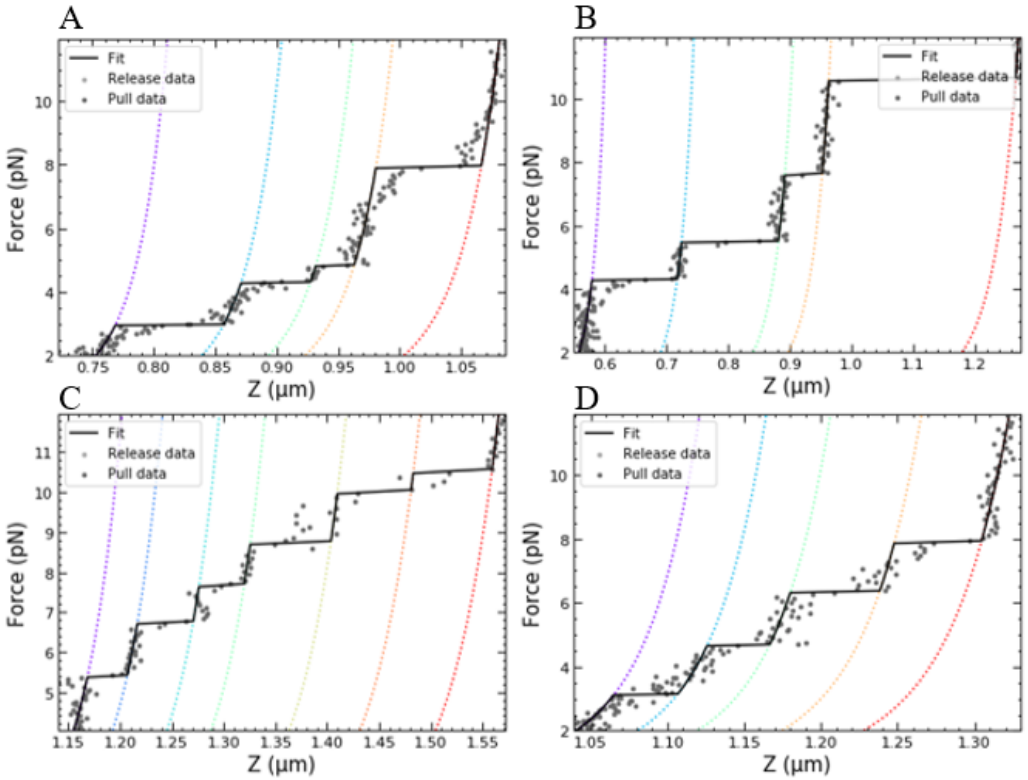

Figure 4.3: *Discrete states can be found with the t-test model (equation 2.15) to describe unstacking behaviour in chromatin fibers with H1. Figures* ***A-D*** *show unstacking of chromatosomes in four independent chromatin fibers. An extendable WLC with the contour length corresponding to a peak in the probability landscape is plotted to confirm the right states are found. Release data are not visible.*

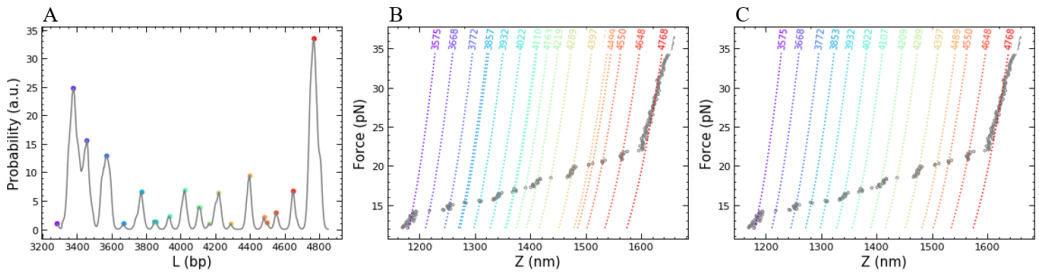

Figure 4.4: *Merging states corrects for wrongly assigned split states.* ***A****: the probability landscape before merging states. Nearby peaks are sometimes identified as seperate states.* ***B****: peaks in the probability landscape are assigned to distinct states. For each peak, a WLC with the corresponding contour length is plotted. Some clusters of datapoints are wrongly assigned to multiple states.* ***C****: after merging states, all groups of datapoints are correctly assigned to their corresponding state.*

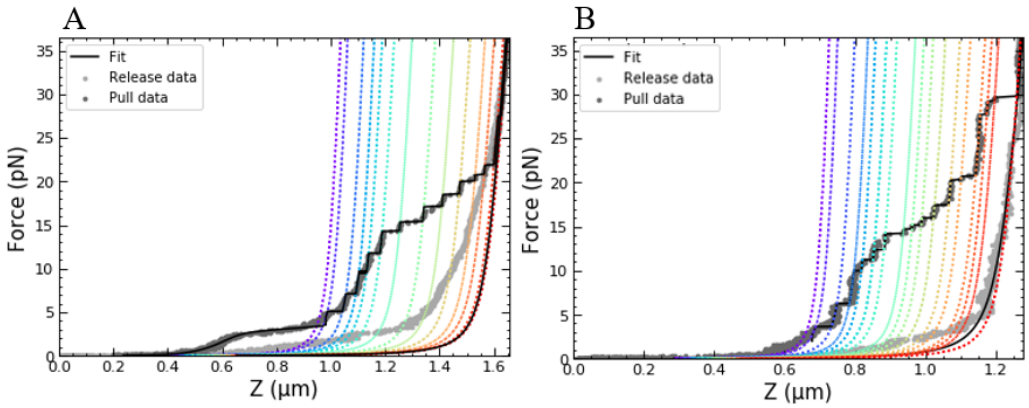

Figure 4.5: *Force-extension curves of chromatin without (****A****) and with (****B****) H1 are qualitatively similar at forces above 10pN, but show different behaviour at forces below 10pN.* ***A****: a force-extension curve of chromatin without H1. Below 10pN, the data was fitted to the equilibrium model with fitting parameters* $N_{tot} = 18.0 \pm 0.1$, $N_{tet} = 4.3 \pm 0.3$, $g_1 = 7.5 \pm 0.2 k_B T$, $k = 0.3 \pm 0.3 pN/nm$ (g_2 *was fixed at* $5.5 K_B T$*). At forces above 10pN, the t-test model was used to identify discrete states corresponding to datapoint clusters.* ***B****: a force-extension curve of chromatin with H1. The WLC curves with contour lengths assigned by the t-test model were joined to describe the entire curve.*

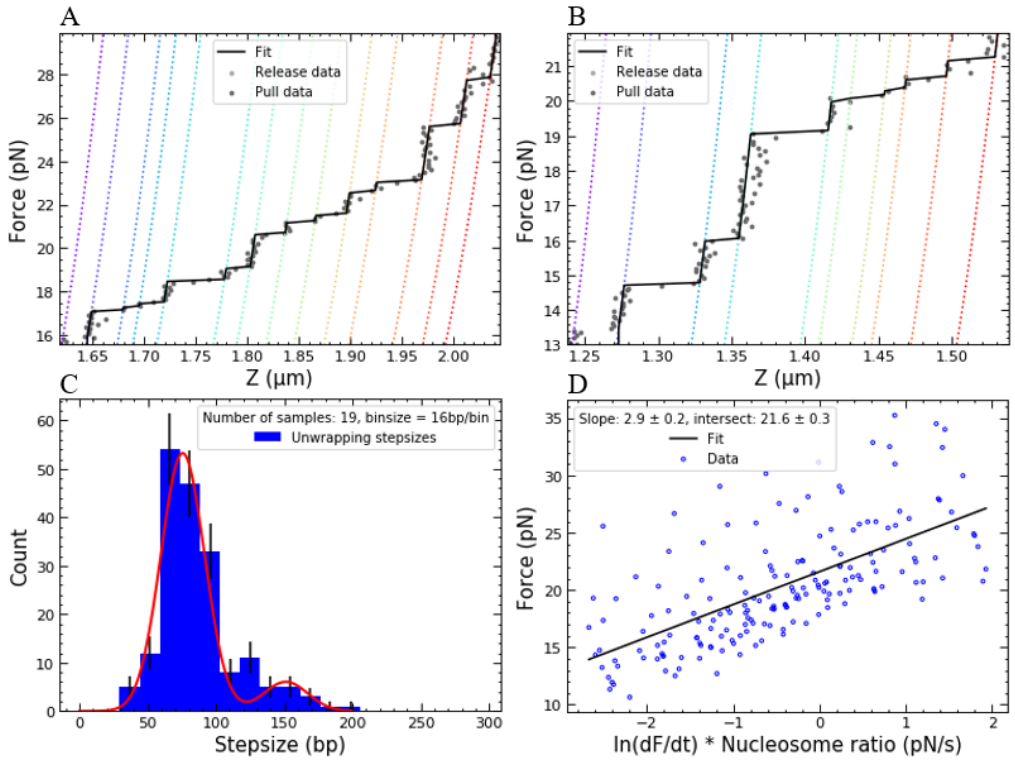

Figure 4.6: *Unwrapping stepsizes in 168NRL chromatin fibers are centered around* $\mu = 75.6 \pm 1.06$ *bp and* $2\mu = 151 \pm 1.05$ *bp.* ***A-B****: identification of discrete unwrapping steps with the t-test model.* ***C****: histogram of the stepsizes with a double Gaussian fit. The second Gaussian represents two nucleosomes unwrapping at the same time.* ***D****: A linear fit of the rupture forces as a function of the logarithm of the pulling rate yields reaction parameters* $\Delta z = 1.4 \pm 0.1\ nm$, $k_0 = 1.90 \pm 0.16 \cdot 10^{-4}\ s^{-1}$, $\Delta G = 31.6 \pm 0.1\ k_B T$. *Release data are not visible.*

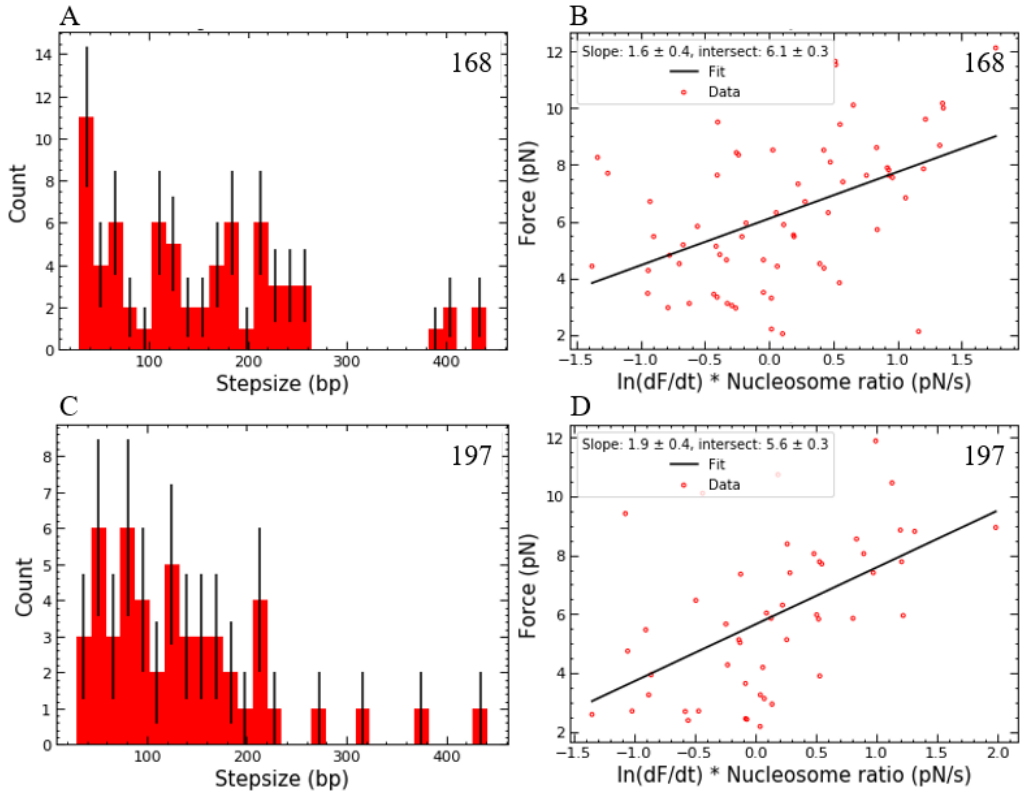

Figure 4.7: *Unstacking stepsizes in 168NRL and 197NRL fibers both vary widely, but reaction parameters show differences.* ***A****: Analysis of the unstacking behaviour of 16 independent 16x168-NRL chromatin fibers with H1 (as shown in figure 4.3) yields a wide variety of stepsizes.* ***B****: A linear fit of the rupture forces as a function of the logarithm of the pulling rate yields parameters* $\Delta z = 2.5 \pm 0.6\ nm$, $k_0 = 1.5 \pm 0.4 \cdot 10^{-2} s^{-1}$, $\Delta G = 27.2 \pm 0.2\ k_B T$. ***C****: Analysis of the unstacking behaviour of 14 independent 16x197-NRL chromatin fibers with H1 (as shown in figure 4.3) yields a wide variety of stepsizes as well.* ***D****: A linear fit of the ruptureforces as a function of the logarithm of the pulling rate yields parameters* $\Delta z = 2.1 \pm 0.5\ nm$, $k_0 = 2.8 \pm 0.7 \cdot 10^{-2} s^{-1}$, $\Delta G = 26.6 \pm 0.2\ k_B T$.

Chapter 5

Discussion

The data collected by doing Magnetic Tweezer experiments on chromatin with and without H1, with NRL's of 168 and 197 confirms a number of statements from previous experiments (1-3), while also providing new insights (4).

1. **At forces below 7 pN, the equilibrium model accurately describes force-extension curves of chromatin without H1.** As described by Meng et al [3], the curves show a plateau at around 3.5 pN. The plateau represents linear extension of the fiber until nucleosome interactions rupture and the outer turn of nucleosomal DNA unwraps from the HO [3]. The values found for g_1 is low ($< 10\,k_BT$) compared to the value of 21.2 k_BT in Meng et al [3]. The found values for g_1 lie closer to the established values for g_1 of a mononucleosome: 8.3 k_BT [3] and 9.0 k_BT [24]. The high-force stepwise unwrapping in figure 4.5A shows that there are more nucleosomes present in the fiber then 601 elements, because each step corresponds to the unwrapping of at least one nucleosome. Meng et al [3] also observed large variations in the low-force regime between individual fibers, which were attributed to variations in fiber compositions. In deed, the number of unwrapping steps varied between 12 and 18 for 16*168NRL reconstituted fibers, indicating a large variation in number of nucleosomes in fibers. This could be explained by dissociation of nucleosomes due to drag forces when flushing the sample into the flowcell. Because the standard errors on the fitted values in the model are low, it can be concluded that the equilibrium model accurately describes chromatin fibers in thermal equilibrium, with large variations in fitted values between fibers.

2. **H1 stabilizes chromatosomes against unstacking.** When H1 is added to chromatin fibers, the regime below $< 10\ pN$ does not show a gradual plateau, but stepwise unstacking of chromatosomes. Individual rupture events can be observed, as opposed to fibers without H1. The difference is shown in figure 4.2. The discrete character of chromatosome unstacking makes it possible to identify the individual unstacking events. There is some variation between different fibers due to the differences in composition, but the final unstacking event lies between 8-10 pN (figure 4.3). For fibers without H1, the plateau associated with similar rupture of nucleosome stacking interactions lies much lower: generally between 3-7 pN (figure 4.2A, [3], [20], [7]). Thus, on average, a higher force is needed to break the nucleosome interactions and unwrap the outer turn of DNA in fibers with H1 opposed to fibers without H1. It can therefore be concluded that H1 stabilizes chromatosomes against unstacking.

3. **Unwrapping stepsizes are normally distributed around** $\mu = 75.6 \pm 1.06\ bp$**.** The non-equilibrium model based on the probability landscape was used to identify stepsizes in low force ($<\ 10\ pN$) unstacking events (figure 4.7) and high force ($>\ 10pN$) unwrapping events (figure 4.6C). A double Gaussian was fitted to unwrapping stepsizes in figure 4.6C to identify two peaks at $\mu = 75.6 \pm 1.06\ bp$ and $2\mu = 151 \pm 1.05\ bp$. The first peak in the distribution can be interpreted as the unwrapping of the remaining 72 bp of nucleosomal DNA from the HO of a nucleosome [4] [25], while the second peak indicates two nucleosomes unwrapping at the same time. The base-pairs are often converted to nanometers, which is not entirely correct since the extension is force-dependent. Here, a value of $0.34\ nm/bp$ is used [30], which yields $\mu = 25.7\ nm$ and $2\mu = 51.3\ nm$. The values found in other experiments vary widely between 22-30 nm [3], which could be attributed to the extra extension that conformation III contributes (figure 2.1). Within a single reconstitution, the value found here is constant as indicated by the small standard error. This suggests conformation III could depend greatly on fiber structure. It can be concluded that unwrapping stepsizes for 16*168 chromatin fibers were found to normally distributed around $\mu = 75.6 \pm 1.06\ bp$. The amount of data in the 2μ region is too low to draw any conclusions with respect to cooperative nucleosome unwrapping.

4. **Difference in 168NRL and 197NRL H1(+) chromatosome unstacking supports difference in nucleosome stiffness.** The model de-

scribed in section 2.2.2 was used to extract reaction parameters from the data. First, the model was pplied to the unwrapping events from figures 4.6A+B. Figure 4.6D shows a linear fit to the data. The average distance the nucleosome stretches before it unwraps the inner turn of nucleosomal DNA was found to be $\Delta z = 1.4 \pm 0.1\ nm$. This is a reasonable value considering the size of the Nucleosome Core Particle [11]. This value is lower than in [4] (3.2 nm) but higher than in [20] (0.8 nm). The difference could be caused by different buffer conditions. The height of the activation barrier was found to be $31.6 \pm 0.1\ kBT$. The height of this barrier further contributes to the stability of the nucleosome at high force. k_0 is low with $1.90 \pm 0.16 \cdot 10^{-4} s^{-1}$, which indicates that inner turn unwrapping rarely occurs spontaneously.
Next, the model was applied to unstacking transitions of 168NRL and 197NRL chromatin fibers with H1. Figure 4.7 shows a wide distribution of stepsizes. Since the uncertainty of the stepsize counts is high, no conclusions can be drawn with respect to the stepsizes. The stretching distance of the nucleosome, Δz, shows no difference within the standard error between 168NRL and 197NRL ($\Delta z_{168} = 2.5 \pm 0.6\ nm, \Delta z_{197} = 2.1 \pm 0.5\ nm$). The height of the activation barrier does show a difference: $\Delta G_{168} = 27.2 \pm 0.2\ k_B T$ and $\Delta G_{197} = 26.6 \pm 0.2\ k_B T$. In deed, it has been suggested by Kaczmarczyk et al [26] that nucleosomes with a short NRL fold into a stiffer structure than nucleosomes with a longer NRL. This would explain the higher activation barrier for 168NRL nucleosomes, since they are folded in a stiffer structure than 197NRL nucleosomes. Moreover, this indicates that the difference in fiber stiffness between 168NRL and 197NRL fibers directly impacts the unstacking parameters. Finally, the value for the transition rate at zero force, k_0, is lower for 168NRL fibers ($k_{0(168)} = 1.5 \pm 0.4 \cdot 10^{-2} s^{-1}$) than for 197NRL fibers ($k_{0(197)} = 2.8 \pm 0.7 \cdot 10^{-2} s^{-1}$), indicating spontaneous unstacking is more likely in 197NRL fibers than in 168NRL fibers. However, since a relatively small amount of data (20 curves per reconstitution) was used, more research is needed to confirm these findings. If confirmed, these findings support the decreasing stiffness for increasing NRL relation found by Kaczmarczyk et al [26], while also demonstrating the difference in fiber stiffness causes a difference in unstacking behaviour in 168NRL and 197NRL chromatin fibers with H1.

Chapter 6

Conclusion

In this thesis, Magnetic Tweezer measurements were done on chromatin fibers with and without adding H1 to obtain force-extension curves. Chromatin fibers with different NRLs were used: 168 and 197.

The flowcell preparation protocol using anti-digoxigenin and BSA was optimalized for DNA to yield the highest percentage of WLC-behaving force-extension curves. It was demonstrated that this protocol also works well for doing measurements on chromatin fibers. However, the yield of curves that could be used for data analysis decreased when measuring the force-extension curves of chromatin. The low yield can be caused by tether ruptures, unwanted surface interactions and excessive forces on the sample during flushing. The yield can possibly be increased by using a different compound for the chromatin binding to the flowcell surface (for example a covalent bond like DBCO [29]). Because this bond is stronger than anti-digoxigenin, ruptures can be reduced. Using different pipette techniques might reduce drag forces on the sample during flushing. Because the statistical relevance of the results depends on the amount of data, more measurements need to be done in order to confirm the four results in this thesis.

The first result shows that the equilibrium model, established by Meng et al [3], describes force-extension curves below 7 pN of chromatin without H1 accurately. The main challenge is to reduce heterogeneity between individual fibers. Because heterogeneity is primariliy caused by structural differences, fibers need to be analyzed seperately to retrieve the exact number of nucleosomes. This is especially important when studying native chromatin, where post-translational modifications can influence unstacking behaviour. Since heterogeneity is also caused by excessive drag

forces during flushing, developing a technique which reduces forces on the chromatin fibers would also increase fiber homogeneity.

The second result indicates that more force is required to unstack nucleosomes in chromatin fiber with H1 than in chromatin fibers without H1. This stabilization has an inhibiting effect on genetic expression, since more force is needed to unfold chromatin fibers with H1 and transcription requires bare DNA. Quantifying this in vivo would be interesting, since the abundancy of chromatosomes is comparable to that of nucleosomes [27]. Furthermore, since different linker histone species affect gene expression in vivo in different ways [28], performing Magnetic Tweezer experiments on chromatin fibers equipped with these subspecies could identify possibly different unfolding characteristics.

The third result confirms that unwrapping stepsizes in chromatin with or without H1 are normally distributed. A peak value of $\mu = 75.6\ bp$ was found, which converted to 25.7 nm was within the range of 22-30 nm found in other experiments [3]. More data is needed for the less-studied second peak, which could support cooperative unwrapping of nucleosomes.

The fourth and final result shows that 168NRL fibers have a higher activation energy barrier and a lower k_0 than 197NRL fibers for unstacking behaviour. This can be explained by the result from Kaczmarczyk et al [26], that the stiffness of fibers with a lower NRL is higher than the stiffness of fibers with a higher NRL. The increased stiffness of the 168NRL fibers would then cause a higher $G^{\dagger}$ and a lower spontaneous unstacking rate k_0. It would be insightful to verify these results by doing force-extension measurements on a variety of fibers with a NRL between 150-200.

Magnetic Tweezers proves to remain a powerful tool to measure force-extension curves of chromatin fibers. The first three results in this thesis confirmed findings of other experiments, added new data, and opened up new suggestions for further research. The final result is new and shows that 168NRL and 197NRL fibers unstack differently. This result provides new insights and suggests new directions for future experiments on chromatin fibers with linker histones.

Acknowledgements

I would like to thank John van Noort for supervising me during this project and giving me valuable feedback and discussions. Chi Pham, thank you for doing chromatin reconstitutions and working on the optimalization of the flowcell protocol with me. I would like to thank the whole van Noort chromatin group for having insightful discussions and giving me an impression of working in a professional research group.

Bibliography

[1] B. Lai, W. Gao, K. Cui, W. Xie, Q. Tang, W. Jin, G. Hu, B. Ni, K. Zhao. *Principles of nucleosome organization revealed by single-cell micrococcal nuclease sequencing.* Nature (2018).

[2] C. Bustamante, S.B. Smith, J. Liphardt, D. Smith. *Single-molecule studies of DNA mechanics.* Curr. Opin. Struct. Biol. (2000).

[3] H. Meng, H. Andresen, J. van Noort. *Quantitative analysis of single-molecule force spectroscopy on folded chromatin fibers.* Nucleic Acids Research (2015).

[4] B. D. Brower-Toland, C. L. Smith, R. C. Yeh, J. T. Lis, C. L. Peterson, M. D. Wang. *Mechanical disruption of individual nucleosomes reveals a reversible multistage release of DNA.* PNAS (2002).

[5] F. Chien. *Chromatin Dynamics resolved with Force Spectroscopy.* PhD Thesis at Leiden University (2011).

[6] N. Ribeck, O. A. Saleh. *Multiplexed single-molecule measurements with magnetic tweezers.* Review of Scientific Instruments 79.9 (2008).

[7] A. Kaczmarczyk. *Nucleosome stacking in chromatin fibers probed with single-molecule force- and torque-spectroscopy.* PhD Thesis at Leiden University (2019).

[8] B. Alberts. *Molecular biology of the cell (4th ed.).* Garland Science. p. 197.

[9] J. T. Finch, A. Klug. *Solenoidal model for superstructure in chromatin.* Proc. Natl. Acad. Sci. U.S.A. 73, 1897−1901 (1976).

[10] R.M. Youngson. *Collins Dictionary of Human Biology.* Glasgow: HarperCollins (2006).

[11] K. Luger, A. W. Mäder, R. K. Richmond, D. F. Sargent, T. J. Richmond. *Crystal structure of the nucleosome core particle at 2.8 A resolution.* Nature. 389 (1997).

[12] K.J. Polach, J. Widom. *Mechanism of protein access to specific DNA sequences in chromatin: a dynamic equilibrium model for gene regulation.* J Mol Biol. (1995).

[13] S.B. Rothbart. *Interpreting the language of histone and DNA modifications.* Biochim Biophys Acta. (2014).

[14] J. Zhou, J.Y. Fan, D. Rangasamy, D.J. Tremethick. *The nucleosome surface regulates chromatin compaction and couples it with transcriptional repression.* Nature Structural Molecular Biology vol. 14, p. 1070−1076 (2007).

[15] J.D. Anderson, J. Widom. *Sequence and position-dependence of the equilibrium accessibility of nucleosomal DNA target sites.* J Mol Biol. (2000).

[16] N. Korolev, A.P. Lyubartsev, L. Nordenskiöld. *A system- atic analysis of nucleosome core particle and nucleosome-nucleosome stacking structure.* Scientific Reports 8.1 p. 1543 (2018).

[17] B.R. Zhou, J. Jiang, H. Feng, R. Ghirlando, T. S. Xiao, Y. Bai. *Structural Mechanisms of Nucleosome Recognition by Linker Histones.* Molecular Cell, Volume 59, Issue 4, p. 628-638 (2015).

[18] R. T. Simpson. *Structure of the chromatosome, a chromatin particle containing 160 base pairs of DNA and all the histones.* Biochemistry 17.25 p. 5524−5531 (1978).

[19] K.W. Jeon, R. Berezney. *Structural and functional organization of the nuclear matrix.* Boston: Academic Press. p. 214â217 (1995).

[20] R. Rodrigues de Mercado. *Quantification of discrete states in chromatin fiber folding.* Bachelor Thesis at Leiden University (2018).

[21] M. Kruithof, F. Chien, M. de Jager, J. van Noort. *Subpiconewton dynamic force spectroscopy using magnetic tweezers.* Biophys. J. 94, p. 2343â2348 (2008).

[22] E. Ben-Haïm, A. Lesne, J. Victor. *Chromatin: a tunable spring at work inside chromosomes.*. Phys. Rev. E , 64 (2001).

[23] R. Janissen. B. Berghuis, D. Dulin, M. Wink, T. van Laar, N. Dekker. *Invincible single molecules: Covalent DNA anchoring strongly enhances the measurable time window and force range.* Nucl. Acids Res. 42 (2014).

[24] S. Mihardja, A.J. Spakowitz, Y. Zhang, C. Bustamante. *Effect of force on mononucleosomal dynamics.* Proc. Natl. Acad. Sci. U.S.A. (2006).

[25] M. Simon, J.A. North, J.C. Shimko, R.A. Forties, M.B. Ferdinand, M. Manohar, M. Zhang, R. Fishel, J.J. Ottesen, M.G. Poirier. *Histone fold modifications control nucleosome unwrapping and disassembly.* Proc. Natl. Acad. Sci. U.S.A. (2011).

[26] A.P. Kaczmarczyk, A. Allahverdi, T.B. Brouwer, L. Nordenskiold, N.H. Dekker, S.J.T. van Noort. *Single-molecule force spectroscopy on histone h4 tail cross-linked chromatin reveals fiber folding*. Journal of Biological Chemistry 292 (2017).

[27] N. Happel, D. Doenecke. *Histone H1 and its isoforms: Contribution to chromatin structure and function.* Gene 431.1-2, p. 1â12 (2009).

[28] R. Alami, Y. Fan, S. Pack, T. M. Sonbuchner, A. Besse, Q. Lin, J. M. Greally, A. I. Skoultchi, E. E. Bouhassira. *Mammalian linker-histone subtypes differentially affect gene expression in vivo.* Proc. Natl. Acad. Sci. U.S.A. (2003).

[29] J. M. Eeftens, J. van der Torre, D. R. Burnham, C. Dekker. *Copper-free click chemistry for attachment of biomolecules in magnetic tweezers.* BMC Biophys. (2015).

[30] G. Damaschun, H. Damaschun, R. Misselwitz, V.A. Pospelov, I.A. Zalenskaya, D. Zirwer, J.J. Müller, V.I. Vorobev. *How many base-pairs per turn does DNA have in solution and in chromatin? An answer from wide-angle X-ray scattering.* Biomed Biochim Acta. (1983).

Chapter 7

Supplementary figures

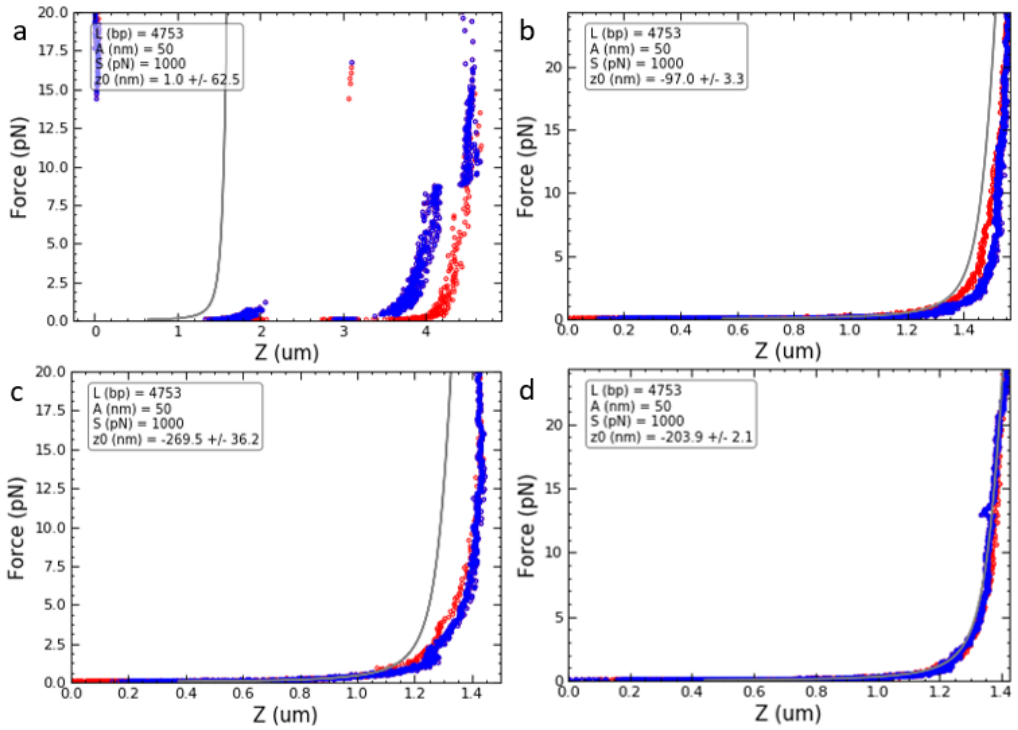

Figure 7.1: *The offset parameter z_0 was used to determine the quality of fit of DNA force-extension curves. Figures* ***A-D*** *show force-extension curves of DNA, with a fitted WLC. Because the DNA tether can bind to multiple locations on the bead, the distance to the flowcell surface can also vary. Therefore, not the DNA contour length is used as fitting parameter but the vertical distance between the lowest point of the bead and the binding site of the tether on the bead. Bead radius (1.4μm) was taken as maximum offset, and the standard deviation for good fits was taken at maximally* 50 *nm. In this figure, only* **A** *does not meet the criteria stated above.*

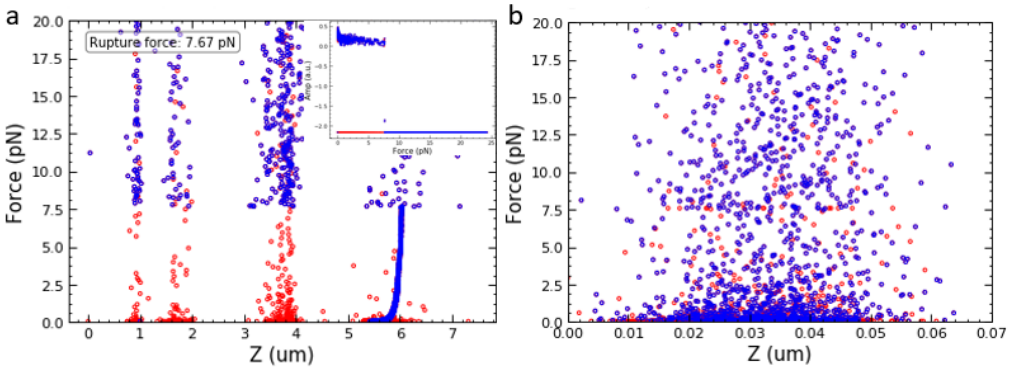

Figure 7.2: *Classification of tether ruptures and stuck beads.* ***A****: a tether was classified as a tether rupture when the peak differential amplitude was greater than 10 times the standard deviation of the derivative of the amplitude, subtracted by the mean of the amplitude. In the right corner of the figure, the corresponding amplitude-force graph is shown.* ***B****: a tether was classified as stuck when the maximum deviation from the mean z-position was no greater than 25 nm.*